



Journal of Quantitative Spectroscopy & Radiative Transfer

Editors-in-Chief: M.P. Mengüç, M.I. Mishchenko and L.S. Rothman

This article was originally published in a journal published by Elsevier, and the attached copy is provided by Elsevier for the author's benefit and for the benefit of the author's institution, for non-commercial research and educational use including without limitation use in instruction at your institution, sending it to specific colleagues that you know, and providing a copy to your institution's administrator.

All other uses, reproduction and distribution, including without limitation commercial reprints, selling or licensing copies or access, or posting on open internet sites, your personal or institution's website or repository, are prohibited. For exceptions, permission may be sought for such use through Elsevier's permissions site at:

<http://www.elsevier.com/locate/permissionusematerial>

Bi-directional reflectance study on particulate layers: Effects of pore liquid absorption coefficient

Kenneth J. Voss*, Hao Zhang

Department of Physics, University of Miami, Miami, FL 33124, USA

Received 25 October 2006; received in revised form 4 January 2007; accepted 5 January 2007

Abstract

We have made bi-directional reflectance distribution function (BRDF) measurements on particulate layers wetted by absorbing liquids. The measurement results indicate that the BRDF tends to become more Lambertian as the interstitial pore liquid becomes more absorbing. The directional hemispherical reflectance, or albedo, of such a layer decreases nonlinearly with a wetting liquid's absorption coefficient. This behavior may be fit by two empirical relationships which independently treat the reflectance from the front surface and reflectance from the bulk material.

© 2007 Published by Elsevier Ltd.

Keywords: Reflectance; Ocean optics

1. Introduction

Most natural particulate surfaces reflect light anisotropically to some extent. This reflectance anisotropy is quantitatively characterized by the bi-directional reflectance distribution function (BRDF) [1]. The BRDF of a natural particulate layer is determined not only by factors such as the optical properties of the individual particles and the packing condition of these particles, including the surface roughness, but also by the surrounding medium's optical properties. For example, a particulate layer wetted with water will, in general, have a darker appearance than the corresponding dry surface [2]. This has been attributed to a decreased refractive index contrast between the particles and the interstitial water [3]. In addition, many shallow water sediment particles may be coated with an extracellular polymeric secretion (EPS) which absorbs strongly and is produced by microbial communities [4]. The BRDF of such a surface may differ noticeably from that of an aggregate of pure sediment grains: a phenomena called the "biofilm gel effect" [4]. Understanding the medium's complex refractive index effect on sediment BRDF will improve our abilities to predict and interpret the benthic environment's light field. Recently we studied the changes in the sediment BRDF induced by wetting the grains with non-absorbing liquids with varied real refractive indices [5]. One of the results of this investigation was that for opaque and lustrous benthic sediment grains, the wetting-induced darkening effect only weakly depends on wetting fluid's refractive index. In this work we investigate the effect of having an

*Corresponding author. Tel.: +1 305 284 2323; fax: +1 305 284 4222.

E-mail address: voss@physics.miami.edu (K.J. Voss).

absorbing wetting liquid on the sediment BRDF. Selected samples are wetted by liquid dye solutions with different absorption coefficients and the BRDF is measured. We will discuss the changes in both the BRDF and reflectance albedo with an absorbing wetting liquid.

2. Experimental method

The BRDF-meter, its calibration, and its data reduction procedures have been described in greater detail previously [6,7]. To summarize, the instrument directs collimated incident irradiance at 0° , 5° , 15° , 25° , 35° , 45° , 55° , and 65° zenith angle and three colors (658, 570, and 475 nm) sequentially onto the sample. Scattered radiance is collected by fiber optics at 107 fixed viewing angles located from 5° to 65° in zenith and from 5° to 345° in azimuth and are imaged as an array on a cooled CCD array camera (Apogee AP 260). Calibration is performed by taking the ratio of the measured reflectance in a given direction to that of a perfect Lambertian diffuser. We present the BRDF data in terms of the reflectance factor (*REFF*) [1] which is defined as the ratio of the bi-directional reflectance of the sample $r(\theta_i, \theta_r, g)$ to that of a perfect diffuser $r_L(\theta_i)$

$$REFF(\theta_i, \phi_i, \theta_v, \phi_v) = \frac{r(\theta_i, \phi_i, \theta_v, \phi_v)}{r_L(\theta_i)} = \frac{r(\theta_i, \phi_i, \theta_v, \phi_v)}{\cos \theta_i / \pi}, \quad (1)$$

where $r(\theta_i, \phi_i, \theta_v, \phi_v)$ is defined as the ratio of the scattered radiance $L(\theta_v, \phi_v)$ and the incident collimated irradiance $E(\theta_i, \phi_i)$, measured perpendicular to the beam

$$r(\theta_i, \phi_i, \theta_v, \phi_v) = \frac{L(\theta_v, \phi_v)}{E(\theta_i, \phi_i)}. \quad (2)$$

r_L is the bidirectional reflectance of a perfect Lambertian reflector,

$$r_L(\theta_i) = \frac{\cos(\theta_i)}{\pi}, \quad (3)$$

and θ_i , ϕ_i , θ_v and ϕ_v are the incident zenith, azimuth, viewing zenith and azimuth angles, respectively. Since we assume our surfaces are azimuthally symmetric, the BRDF data are dependent only on the difference, $|\phi_i - \phi_v| = \phi$. The bi-directional reflectance quantities can also be expressed in terms of the phase angle g defined by

$$\cos g = \cos \theta_i \cos \theta_v + \sin \theta_i \sin \theta_v \cos(\phi_v - \phi_i). \quad (4)$$

The direction of $g = 0$ corresponds to the exact backscattering direction and large g ($g > 90^\circ$) corresponds to the forward scattering direction. The *REFF* will be displayed versus g throughout this work. Positive phase angles correspond to $0^\circ \leq \phi \leq 180^\circ$ and the negative phase angles correspond to $-180^\circ \leq \phi \leq 0^\circ$. For a perfect surface, the *REFF* should be totally symmetric about the plane of incidence, however, for real particulate surfaces, differentiating between the two sides allows us to test the uniformity of the surface. Asymmetries can be traced to problems with the surface geometry. Note that since we are looking at reflected light, we are restricted to $\theta_v < 90^\circ$. If θ_i is zero, $g = \theta_v$, and is less than 90° , if θ_i is greater than zero, larger g values can be measured.

The directional albedo \tilde{r} of a particulate surface may be obtained by integrating the *REFF* over the upper hemisphere as [8]

$$\tilde{r}(\theta_i) = \pi^{-1} \int_{2\pi} \int_{\pi/2} REFF(\theta_i, \theta_v, \phi) \cos \theta_v \sin \theta_v \, d\theta_v \, d\phi. \quad (5)$$

According to Hapke [1], the directional albedo at 60° -incidence may be used to approximate the diffusive reflectance r_0 , which is defined as the ratio of the total scattered power emerging in all upward directions from a unit area of the surface to the total power incident on the surface per unit area. One of the advantages of using diffusive reflectance is that, under certain assumptions, it can be used to estimate the absorption coefficient of the individual grains in a particulate layer [1].

In this paper we concentrate on BRDF measurements taken with illumination at 658 nm for three reasons. First, we have found that the angular variation of the BRDF for the sediment samples we have measured are

at most only weakly wavelength-dependent in the visible; second, the red light has the highest signal-to-noise ratio in our BRDF-meter and third, the blue dye we use in this work strongly absorbs red light. Since the shape of the sediment BRDF is mostly wavelength independent, this work can be extended to other wavelengths with an appropriate change in the absorption coefficient.

Samples used in this work include benthic sediment particle ooids collected from near Lee Stocking Island, Exumas, Bahamas during the summer 2000, and beach sand collected from Crandon Beach, Miami (*Crandon*) [5]. The ooids have a lustrous and smooth surface and have been found to have an albedo change of only 10% upon wetting [5]. We chose two size distributions for ooids; diameters between 0.25 and 0.5 mm (*sediment A*), and between 0.5 and 1 mm (*sediment B*).

The wetting liquid used was tap water with varied concentrations of gel food color (blue, Betty Crocker). The absorption coefficient of the liquid at the BRDF-meter's red LED wavelength 658 nm, α^{658} , was estimated by the following method. First, we measured the transmission at 633 nm through a 1 cm cuvette of dye solution and a water sample, i.e.,

$$\alpha^{633} = -\ln \left[\frac{I^{\text{sol}}}{I^{\text{Wat}}} \right]. \quad (6)$$

Fig. 1 shows α^{633} versus dye weight concentration with the linear fitting result

$$\alpha^{633}(\text{cm}^{-1}) \approx 32.8 \times \text{wt}\%. \quad (7)$$

We neglect any scattering effect over the 1 cm path length and specify the absorption coefficient of water to be 0 when wt% is 0. Note that all of the dye solutions used had $\alpha^{633} > 25 \text{ m}^{-1}$, thus the dye absorption was much larger than the water solvent. This expression was used to obtain the absorption coefficient of the wetting liquid including the cases where the samples were too absorbing to be measured by the transmission method. Then we measured the spectral absorbance (200–1100 nm) of two typical dilute gel solutions on an Agilent 8453 Spectrometer. With the spectral absorbance A defined by

$$A = -\log \left[\frac{I^{\text{sol}}}{I^{\text{Wat}}} \right], \quad (8)$$

we get

$$\alpha = A \ln 10. \quad (9)$$

With this relationship and the measured spectral absorbance we can easily scale α^{633} to α^{658} . Since the red LED has a FWHM of 24 nm [6], we integrated over a Lorentzian lineshape to obtain the average absorption coefficient at 658 nm.

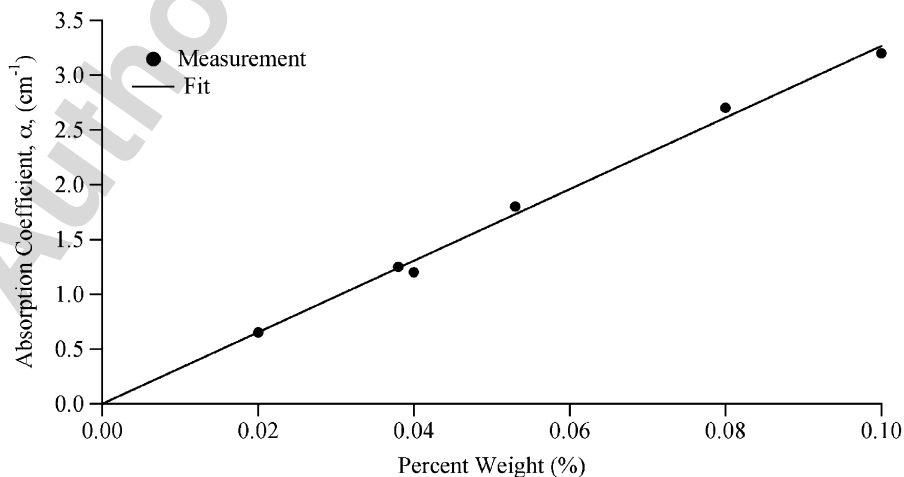


Fig. 1. The relationship between the absorption coefficient at 633 nm, α^{633} , and the dye weight concentration.

3. Result and discussion

3.1. Sediment A and Sediment B

These two samples were wetted by nine dye solutions (in addition to water) with absorption coefficients between 0.254 and 40.80 cm^{-1} . Fig. 2(a) and (b) show the *REFF* for *Sediment A* when dry, water wetted, and wetted by three typical absorbing solutions at normal and 65° incidences, respectively. At normal incidence (Fig. 2(a)) the following features are clearly seen: when going from dry to wet, the *REFF* decreases by approximately 15% and becomes less anisotropic. When the absorption coefficient of the wetting liquid increases, the *REFF* decreases and becomes more Lambertian until at very large absorption (40.80 cm^{-1}) the *REFF* shows a feature that the nadir values are lower than those at larger viewing angles by 5%. To better manifest this feature we normalize the *REFF* to the value at a minimum phase angle. Specifically, for normal

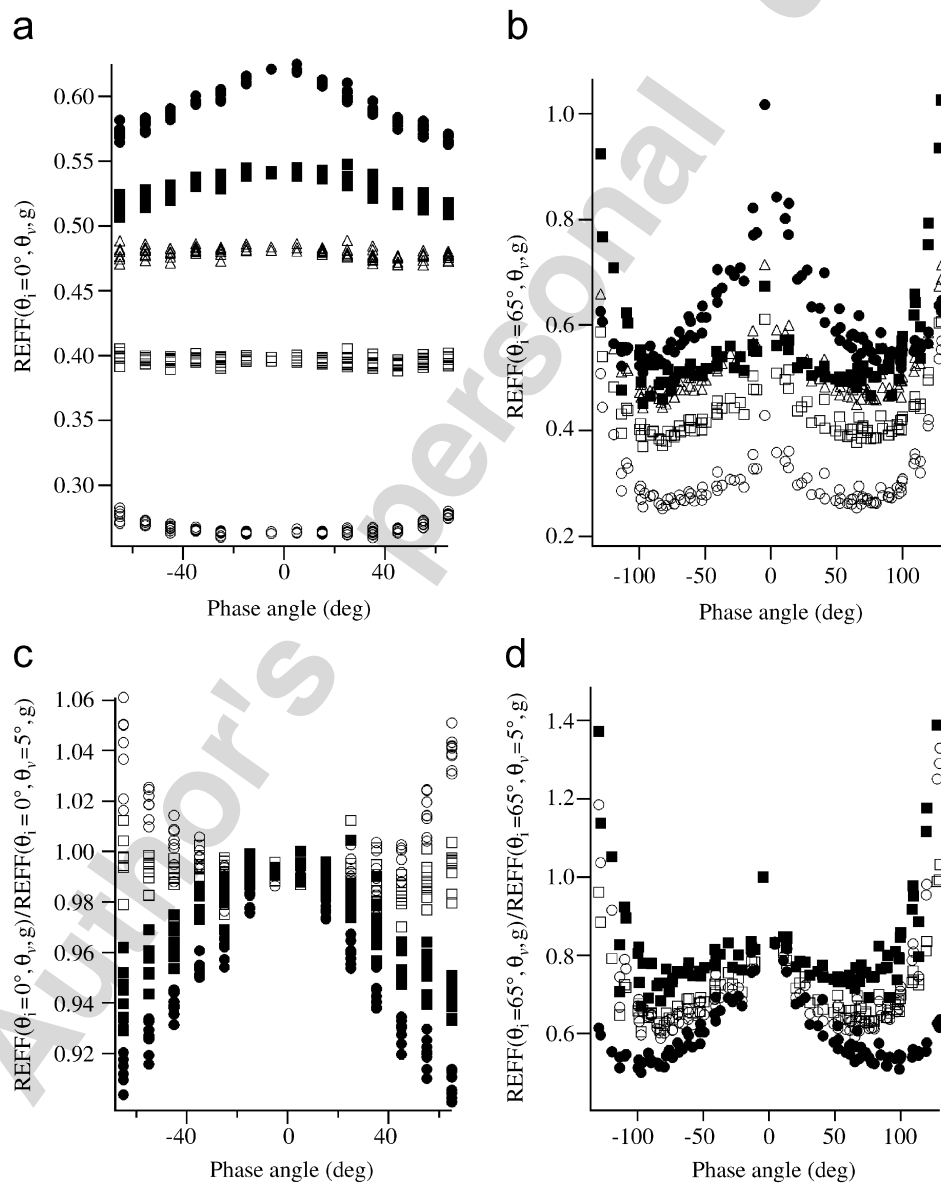


Fig. 2. The REFF of *Sediment A* when dry, wetted with water and wetted with three absorbing solutions. (a) 0° -incidence (b) 65° -incidence (c) normalized 0° -incidence and (d) normalized 65° -incidence. Filled circles—dry; filled squares—water wetted; open triangles— $\alpha^{658} = 2.54 \text{ cm}^{-1}$; open squares— $\alpha^{658} = 10.5 \text{ cm}^{-1}$; open circles— $\alpha^{658} = 40.8 \text{ cm}^{-1}$. For clarity, the $\alpha^{658} = 2.54 \text{ cm}^{-1}$ data are not shown in (c) and (d).

incidence we picked up a viewing fiber located at 5° zenith and -135° azimuth which gives a phase angle of 5° (for 65° incidence, we picked up the fiber at 65° zenith and -5° azimuth which gives a phase angle -4.5°). It should be noted that although there is typically a 1% variation between the five viewing fibers with phase angle 5° on a particulate surface at normal incidence, it does not make a significant difference in demonstrating the normalized *REFF* features. Fig. 2(c) and (d) show the normalized *REFF* at normal and 65° incidence, respectively. At normal incidence and high absorption the normalized data shows that the *REFF* increases drastically as the phase angle increases. This is the first time we have seen such a large *REFF* relative to nadir in our field or laboratory BRDF data. At normal incidence there is also no evidence of a hotspot when the absorption coefficient is this large.

At 65° -incidence, wetting by water makes the *REFF* forward scattering in contrast to the backscattering dry *REFF*; however, increasing the absorption coefficient of the wetting liquid only seems to lower the overall *REFF* values and preserves the angular pattern (Fig. 2(b) and (d)).

Fig. 3 displays similar results for *sediment B*. From Fig. 3 one can see that both the wetting and the absorption coefficient effects are similar to *sediment A* (Fig. 2). The differences are that at 65° -incidence all normalized *REFF*'s lie almost on top of each other and the overall *REFF*'s are lower than that of *sediment A*. With larger grain size sediments, the reflectance tends to decrease [9] and we have seen that surface effects dominate, particularly at larger incident angles. It appears that the angular structure is dominated by the first surface while the overall magnitude of the *REFF* contains a diffuse component which is reduced with increasing absorption coefficient.

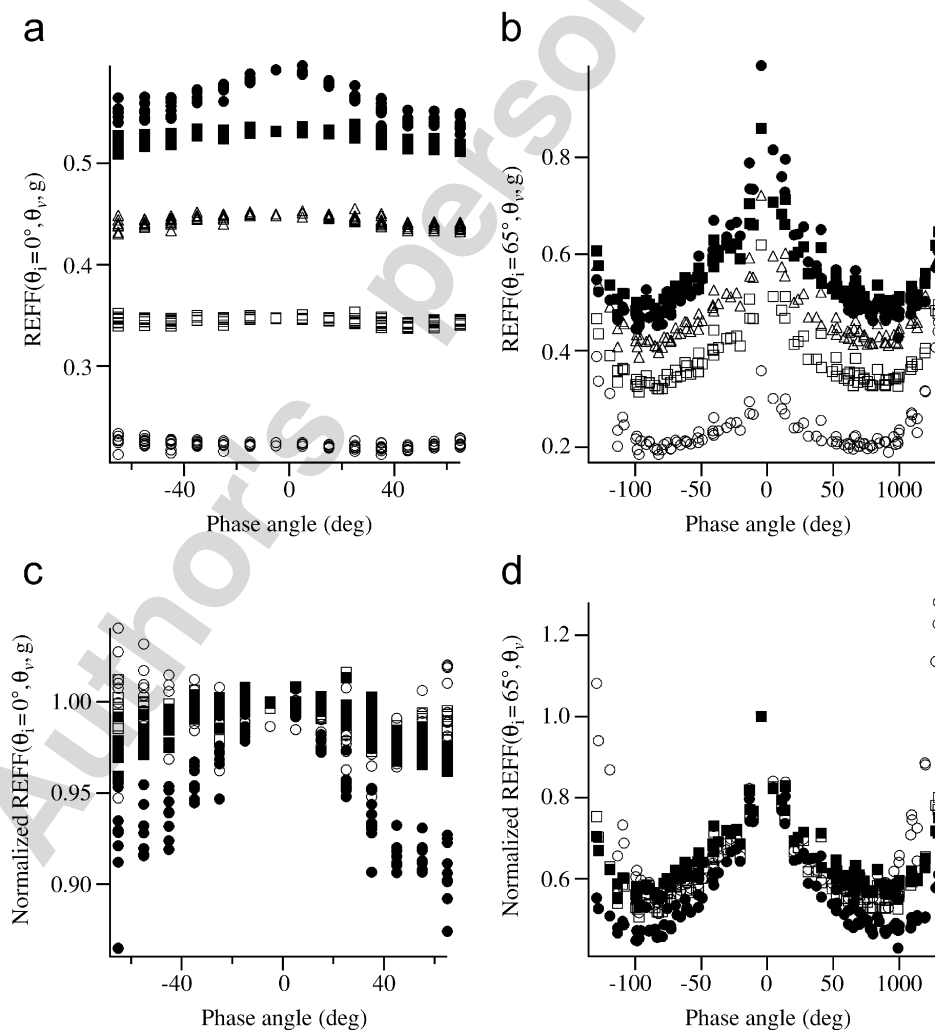


Fig. 3. Same as Fig. 2, but for *Sediment B*.

3.2. Crandon

Sediment A and *sediment B* shown above are opaque shallow water sediments with no translucent particles. Since we have found that the more translucent particles a particulate layer has, the stronger its wetting-induced BRDF change [5], it would be interesting to see if the effects seen in the ooids exist in beach sands containing transparent grains. We chose *Crandon* which contains about 36% translucent quartz-like grains and has been found to have the greatest wetting-induced darkening effect [5]. Fig. 4 is the typical $REFF$ and normalized $REFF$ at normal and 65° incidences. From Fig. 4 one can see that the additional darkening effect caused by absorbing liquids is not as significant as in *sediment A* and *sediment B*. This is because when going

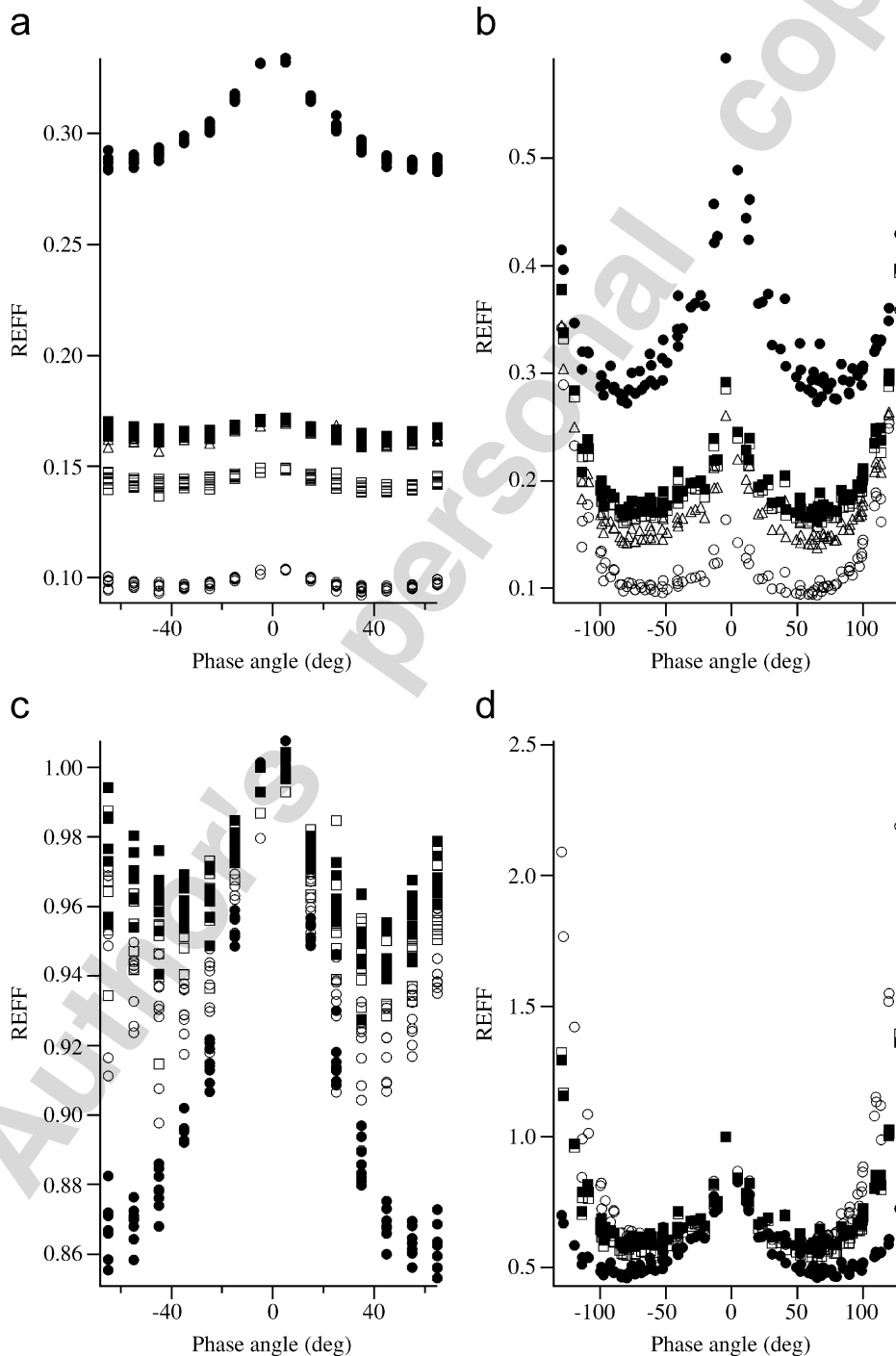


Fig. 4. Same as Fig. 1, but for *Crandon*.

from dry to water wetted, the surface brightness has already been reduced by nearly 50%, and thus wetting the surface with more absorbing solutions does not cause as great an additional effect as in *sediment A* and *sediment B*.

3.3. Discussion

To investigate the relationship between the surface brightness and wetting liquid absorption coefficient, we plot the diffusive reflectance r_0 (directional albedo at 60° -incidence) versus the wetting liquid absorption coefficient for both *sediment A* and *sediment B*, and that for *Crandon* in Fig. 5. Since the BRDF-meter does not have an incident illumination at 60° , we fit a curve to the directional albedo versus the incident zenith angle and interpolate to obtain the albedo value at 60° . It is seen that for both *sediment A* and *sediment B* the diffuse reflectance reduction is nearly 50% over the absorption coefficient range and decreases very nonlinearly with the wetting liquid absorption coefficient; for *Crandon*, the reduction is only very small. As mentioned above, the *Crandon* sample contains translucent grains and thus wetting with water has a large effect on the albedo; absorbing liquids do not seem to decrease the surface brightness as much but the behavior is similar.

3.3.1. Simple reflectance models

Two simple models can describe the behavior of r_0 versus α . The first model assumes that the reflectance is due to a summation of reflectance from the layers of sediment grains, separated by some absorbing liquid. In this model, the front surface of the first layer is specified to be R_S , and each of the following surfaces reflects a portion of the incident light, R_0 . Separating R_S and R_0 accounts for the difference in R due to the different radiance distribution hitting the surface, R_S for more collimated incident light and R_0 for the more diffuse incident light. The transmission to the next layer, T , is given by

$$T = e^{-d\alpha}, \quad (10)$$

where d is the distance between effective layers and α is the absorption coefficient. The summation of all the terms, due to the different layers, leads to

$$r_0 = R_S + \frac{(1 - R_S)(1 - R_0) e^{-2d\alpha} R_0}{1 - (1 - R_0)^2 e^{-2d\alpha}}. \quad (11)$$

When α gets large this converges to R_S , the value of r_0 from just the first surface. Fitting this equation to the two data sets, one obtains for *sediment A*: $R_S = 0.26 \pm 0.02$, $R_0 = 0.39 \pm 0.05$, and $d = 220 \pm 60 \mu\text{m}$.

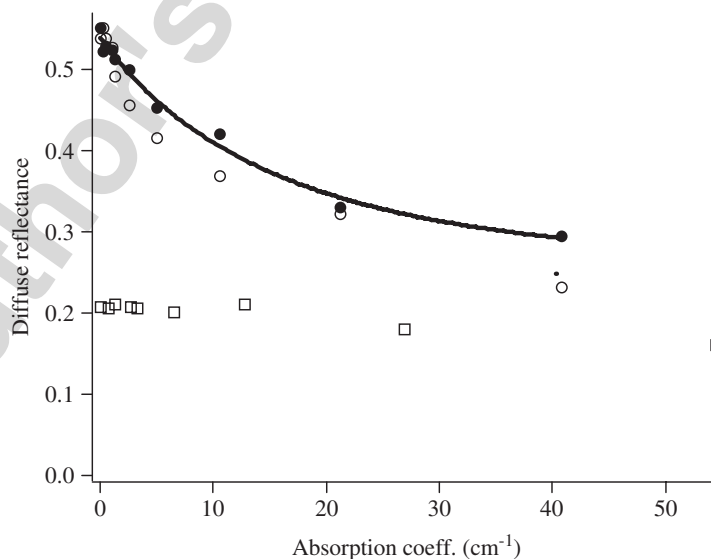


Fig. 5. Comparisons of the diffusive reflectance (albedo at 60° -incidence zenith) with simple model 1 as described in text, for *Sediment A* (filled circles), *Sediment B* (open circles) and *Crandon* (open squares). Line is the result of a fit with a simple model as described in the text. Solid line is fit to *Sediment A*, dotted line is fit to *Sediment B*.

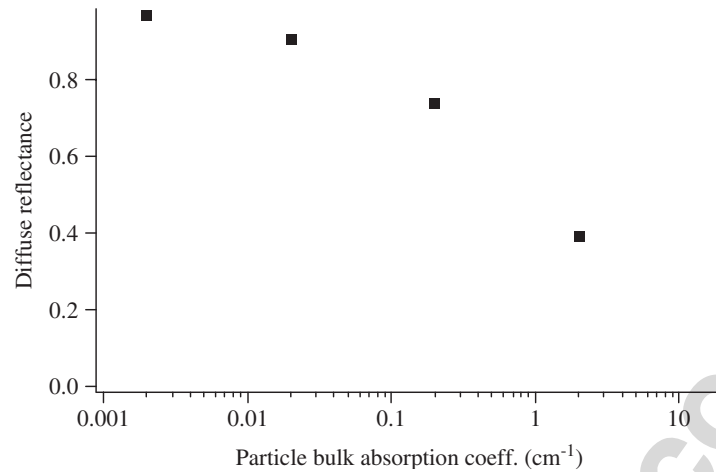


Fig. 6. Diffuse reflectance (albedo at 60°-incidence) calculated by RTE model versus the particle bulk absorption coefficient. The particles are spherical grains having a power law size distribution with mean radius of 100 μm and a variance of 0.1. The real refractive index is 1.2 and the imaginary index is varied from 10^{-8} to 10^{-4} .

For *Sediment B* the parameters are $R_S = 0.22 \pm 0.04$, $R_0 = 0.029 \pm 0.08$, and $d = 240 \pm 100 \mu\text{m}$. The results are shown in Fig. 5.

A similar fit can be obtained by assuming the reflectance is made up of two parts, a diffuse component from the bulk material, and a component from the first surface:

$$r_0 = R_1 + R_2 e^{-d\alpha}. \quad (12)$$

This is particularly attractive from when considering earlier work of the *REFF* of spheres, which had a large single scattering signature over a diffuse background [10]. Fitting with this equation, for Sample A, leads to: $R_1 = 0.28$, $R_2 = 0.26$, and $d = 670 \mu\text{m}$. For Sample B this is: $R_1 = 0.24$, $R_2 = 0.30$, and $d = 880 \mu\text{m}$. This model fit is very close to that of Model 1 and thus is not shown in Fig. 5.

It is interesting to note that the behavior of r_0 versus α observed in this work is similar to the effect which would occur with an increase in the particulate bulk absorption coefficient. To demonstrate this, in Fig. 6 we plot the albedo at 60°-incidence of a particulate layer with infinite optical thickness against the particle bulk absorption coefficient s ($s = 4\pi k/\lambda$ with k the imaginary refractive index). The individual particles in the layer are assumed to be spherical having a power law size distribution [11] with mean radius of 100 μm and a variance of 0.1 under 633 nm incidence. The real refractive index is 1.2 ($= 1.6/1.33$) and the imaginary refractive index is varied from 10^{-8} to 10^{-4} . The directional albedos are calculated by radiative transfer algorithms [12,13]. By comparing Fig. 6 with Fig. 5 we feel that it would be difficult to separate the effects of particle bulk absorption coefficient and the pore liquid absorption coefficient from the albedo data alone.

4. Conclusions

In brief, this work has demonstrated that the BRDF of typical sediment particles surrounded by absorbing liquids differ significantly from both the dry and water-wetted layers. The overall effects of wetting with an absorbing liquid are to decrease the albedo and make the surface appear more Lambertian. We have also found that at normal incidence when the absorption coefficient is very large the BRDF can be bowl shaped, which has not been found in our other measurements of natural samples. For both shallow water sediments, which are totally opaque grains, and beach sands having translucent particles, the surface albedo decreases nonlinearly as the wetting fluid absorption coefficient increases. Simple empirical relationships can be fit to this decrease. It is important to note that, since the first few layers of a sediment determine the *REFF* and albedo of a surface, that the absorption coefficient of the interstitial material must be very high (on the order of 100 s m^{-1}) to have a significant effect. Thus it is unlikely that the albedo, or *REFF*, of a surface would provide unambiguous information on the absorption coefficient of the liquid in a natural sediment.

Conversely, except in extra-ordinary situations, one need not consider the absorption coefficient of the interstitial liquid when modeling or predicting the reflectance from natural surfaces.

Acknowledgment

This work was supported by the Ocean Optics program at the Office of Naval Research.

References

- [1] Hapke B. Theory of reflectance and emittance spectroscopy. New York: Cambridge University; 1993.
- [2] Bohren CF. Clouds in a glass of beer—simple experiments in atmospheric physics. New York: Wiley; 1987.
- [3] Twomey SA, Bohren CF, Mergenthaler JL. Reflectance and albedo differences between wet and dry surfaces. *Appl Opt* 1986;25:431–7.
- [4] Decho A, Kawaguchi T, Allison MA, Louchard EM, Reid RP, Stephens FC, et al. Sediment properties influencing upwelling spectral reflectance signatures: the biofilm gel effect. *Limnol Oceanogr* 2003;48:431–43.
- [5] Zhang H, Voss KJ. Bi-directional reflectance study on dry, wet and submerged particulate layers-effects of pore liquid refractive index and translucent particle concentrations. *Appl Opt* 2006;45:8753–63.
- [6] Voss KJ, Chapin AL, Monti M, Zhang H. Instrument to measure the bidirectional reflectance distribution function of surfaces. *Appl Opt* 2000;39:6197–206.
- [7] Voss KJ, Zhang H. Bi-directional reflectance of dry and submerged Labsphere Spectralon plaque. *Appl Opt* 2006;45:7924–7.
- [8] Zhang H, Voss KJ, Reid RP. Determining the influential depth of sediment particles by BRDF measurements. *Opt Express* 2003;11:2654–65.
- [9] Bohren CF. Multiple scattering and some of its observable consequences. *Am J Phys* 1987;55:524–33.
- [10] Zhang H, Voss KJ. Comparisons of BRDF Measurements on prepared particulate surfaces and radiative transfer models. *Appl Opt* 2005;44:597–610.
- [11] Mishchenko MI, Travis LD, Lacis AA. Scattering, absorption, and emission of light by small particles. New York: Cambridge University; 2002.
- [12] Mishchenko MI, Dlugach JM, Yanovitskij EG, Zakharova NT. Bidirectional reflectance of flat, optically thick particulate layers: an efficient radiative transfer solution and applications to snow and soil surfaces. *JQSRT* 1999;63:409–32.
- [13] Stamnes K, Tsay SC, Wiscombe W, Jayaweera K. Numerically stable algorithm for discrete-ordinate-method radiative transfer in multiple scattering and emitting layered media. *Appl Opt* 1988;27:2502–9.